Proceedings of The National Conference
On Undergraduate Research (NCUR) 2013
University of Wisconsin La Crosse, WI
April 11–13, 2013

On the determination of photo-actuation effects for a polymer/MWCNT composite fiber based cantilever

Aixa de Jesús Espinosa
Department of Mathematics
University of Puerto Rico at Humacao
Humacao, PR 00792

Faculty Advisor: Pablo Negrón

Abstract

Carbon Nanotubes can be used in a wide range of applications due to their outstanding physical properties. Some of the applications are as sensors and actuators. A novel photo actuation mechanism has been reported for polymer-carbon nanotube composites. This unusual quality is favorable in the development of new and better microelectronic devices, like in Braille displays, artificial muscles, and drug delivery. Composite fibers combining Multi Wall Carbon Nanotubes (MWCNT) and Sodyum dodecyl sulfate (SDS) have been produced in the laboratory by the electro–spinning technique. These fibers exhibit photo-actuation properties when exposed to an external light source. To study this phenomenon, we use a model from nonlinear elasticity to determine the forces and internal torques on a given fiber that were induced by the photo actuation effect. We use an inverse method in which starting from a digitized picture of the deformed fiber, we construct using splines a function describing the deformation of the fiber. Using this function we can determine the coefficients in the equations of equilibrium for the fiber, from which the corresponding forces and torques are calculated. This method is used to study the effects of the cross sectional geometry of the fibers on the induced body forces and torques.

Keywords: Photo-actuation, composite fibers, inverse method, cantilever

1. Introduction

On-going efforts to produce novel materials with improved or augmented functionalities as sensors and actuators frequently focus in smart materials. Smart materials respond to external stimuli in a controlled fashion. Amongst these, stimulus-active polymers (and polymeric composites) are the subject of recent discussion. Indeed, the possibility of microsystem integration and of biocompatibility has opened the door to actuators in Braille displays[10], artificial muscles[4], and drug delivery. In the recent literature, a number of studies have reviewed the current state of the art in shape-memory polymers responsive to a variety of stimuli (heat, light, magnetic and electric fields, and water/solvent media)[9,5], addressing physical mechanisms inherent to actuation. Historically, thermally-activated shape-memory polymers were first studied and several activation mechanisms have been documented, such as melting transition or in-direction heating amongst others[9]. Mostly, the physics behind the actuation can be explained by the capacity of the polymer (or polymeric composite), with negligible internal stress in the original state, to store mechanical deformation at lower temperatures. Upon increased temperature, temporary cross-links release mechanical stress, leading to recovery of the original shape[5]. Electroactive polymers possibly second their thermoactive counterparts in technological advancement. Two activation mechanisms prevail: field actuation and ionic diffusion[4]. In field-activated systems, a Coulomb electrostatic field induces conformational changes by dipole aligning and ionic electroactive polymers involve ion diffusion upon field activation; where the macroscopic motion of charged species is responsible for actuation.

A novel actuation mechanism has been reported for polymer-carbon nanotube composites[1,2]. In this scheme, irradiation of a source with distribution centered at 675 nm promotes actuation stresses of up to 100 kPa. Although

the temperature during actuation increases by ~15ºC, thermal saturation occurs after a few minutes of irradiation, therefore dismissing heat as trigger. In addition, the photomechanical response of MWCNTs embedded in a silicon rubber PDMS matrix is a new effect not associated to a magnifying mechanism due to the presence of MWCNTs, as the pristine elastomer shows a minimal response to the same irradiation source due to heating. Although both expansion and contraction-actuation modes are possible (arguably, depending on the degree of alignment due to pre-applied strains), the magnitude of the stroke depends solely on the matrix, suggesting the possibility of photoactuation as a universal phenomenon in polymer-MWCNT composites. These are promising characteristics for microelectronic applications, where fast, reversible actuation is preferred for instance, to thermally-induced processes.

Composite fibers combining MWCNT and Sodyum dodecyl sulfate (SDS) have been produced in the laboratory by the electro-spinning technique. These fibers exhibit photo-actuation properties when exposed to an external light source[8]. In this paper we employ a model from nonlinear elasticity to describe the deformation of a given fiber and for computing the forces and internal torques that induce the photo-actuation effect. We use an inverse method in which starting from the known deformation of the fiber, obtained from digitized pictures of the bended fiber, the corresponding forces and torques are calculated.

2. The Mathematical Model: The Inverse Problem

The discussion in this section is based on the presentation in[3] where more details and generalizations of the theory are discussed. The article in[7] contains a similar discussion.

In the Cosserat special theory, a planar configuration of a column or rod can be described with two functions:

$$\mathbf{r}, \mathbf{b} : [0, L] \to \text{span}\{\mathbf{i}, \mathbf{j}\}.$$

The unit vector $\mathbf{b}(s)$ is called the directrix at s. If we define the unit vector $\mathbf{a} = -\mathbf{k} \times \mathbf{b}$, then $\mathbf{a}, \mathbf{b} \in$ span $\{\mathbf{i}, \mathbf{j}\}$ and are orthogonal. Hence there exists a function $\theta(s)$ such that:

$$\mathbf{a}(s) = \cos\theta(s)\mathbf{i} + \sin\theta(s)\mathbf{j}, \quad \mathbf{b}(s) = -\sin\theta(s) + \cos\theta(s)\mathbf{j}.$$

Since $\{\mathbf{a}, \mathbf{b}\}$ is a base for span $\{\mathbf{i}, \mathbf{j}\}$, we can write:

$$\mathbf{r}'(s) = v(s)\mathbf{a}(s) + \eta(s)\mathbf{b}(s),$$

for some functions $v(s)$, $\eta(s)$. These functions together with $\mu(s) = \theta'(s)$ are called the *strains* and they completely characterize the deformation of the column. To ensure that the deformation of the bar is not so severe as to make **r** y **b** parallel, we require that:

$$v(s) > 0, \quad s \in [0, L].$$

We assume that the material of the bar is inextensible and unshearable. In terms of the strains, this is equivalent to:

$$v(s) = 1, \quad \eta(s) = 0, \quad \forall s \in [0, L].$$

Let $(\mathbf{f}(s), l(s))$ be the external (body) force and torque per unit length respectively, and $\hat{M}(\mu(s), s)$ the contact bending couple. If we define $\mathbf{c}(s) = c_1(s)\mathbf{i} + c_2(s)\mathbf{j} = \int_s^L \mathbf{f}(t)\mathrm{d}t$, then we have now[3] that the equations of equilibrium of the bar are given by:

$$\frac{d}{ds}\left[\hat{M}(\theta'(s), s)\right] - c_1(s)\sin\theta(s) + c_2(s)\cos\theta(s) + l(s) = 0, \qquad 0 < s < L, \tag{1}$$

subject to the boundary conditions:

$$\theta(0) = 0, \quad \theta'(L) = 0.$$

For given functions $c_1(s), c_2(s), l(s)$, this equations yield a boundary value problem for the function $\theta(s)$. This boundary value problem is called the *direct problem*.

In the *inverse problem*, we assume that the functions $c_1(s), c_2(s), l(s)$ are unknown, with $\theta(s)$ known or given. This problem in general has no solution, and when it does, it may not be unique. In this paper we consider the special case in which $c_1(s) = 0$ and $l(s) = l = \text{constant}$. With these assumptions, equation 1 reduces to:

$$\frac{d}{ds}\left[\hat{M}(\theta'(s), s)\right] + c_2(s)\cos\theta(s) + l = 0. \tag{2}$$

If $\theta(s)$ is known, we can use this equation to get $c_2(s)$ and l.

4. The Numerical Scheme

The numerical scheme for the solution of the inverse problem consists of two parts:

i) using the laboratory data about the deformation of the fiber, we find approximations for the function $\theta(s)$ and its derivative.

ii) With the information about $\theta(s)$ obtained in the first part, we compute approximations for the function $c_2(s)$ using the differential equation (2) and boundary conditions.

For the theory and error analysis about the numerical techniques used in this section, we refer for instance to[6].

4.1 approximation of $\theta(s)$ and

We assume that the information about the deformation of the fiber is given in terms of the data points:

$$\{(x_i, y_i) : 1 \le i \le n\},$$

where the x_i's are not necessarily uniformly spaced. Define the mid-points of the intervals $[x_i, x_{i+1}]$, $1 \le i \le$ n - 1, by

$$x_{i+\frac{1}{2}} = \frac{x_i + x_{i+1}}{2}, \quad 1 \le i \le n-1.$$

For any function $g(x)$, we write g_i or $g_{i+½}$ to denote any approximation of $g(x_i)$ or $g(x_{i+½})$ respectively.
Define

$$y'_{i+\frac{1}{2}} = \frac{y_{i+1} - y_i}{x_{i+1} - x_i}, \quad 1 \le i \le n-1.$$

Since the function θ represents the angle that the tangent to the deformed curve makes with the horizontal, we have that

$$\theta_{i+\frac{1}{2}} = \tan^{-1}\left[y'_{i+\frac{1}{2}}\right], \quad 1 \le i \le n-1.$$

Hence we can take

$$\theta_i = \frac{\theta_{i-\frac{1}{2}} + \theta_{i+\frac{1}{2}}}{2}, \quad 2 \le i \le n-1.$$

The boundary condition $\theta(0) = 0$ is incorporated by taking $\theta_1 = 0$, while $\theta'(L) = 0$ leads to the condition $\theta_n = \theta_{n-1}$. To approximate the derivatives of θ as a function of s (the arc-length), we introduce the approximate arc-length function given by:

$$s_1 = 0, \quad s_i = \sum_{k=1}^{i-1} (x_{k+1} - x_k) \sqrt{1 + \left(y'_{k+\frac{1}{2}} \right)^2}, \quad 2 \le i \le n.$$

We now have that

$$\theta'_i = \frac{\theta_{i+\frac{1}{2}} - \theta_{i-\frac{1}{2}}}{s_{i+\frac{1}{2}} - s_{i-\frac{1}{2}}}, \quad 2 \le i \le n-1.$$

Using that $\theta'(L) = 0$, we set $\theta'_n = 0$. For the approximation θ'_1, we construct the linear polynomial that interpolates the data (s_2, θ'_2), (s_3, θ'_3), and then extrapolate to $s_1 = 0$:

$$\theta'_1 = \theta'_2 - s_2 \frac{\theta'_3 - \theta'_2}{s_3 - s_2}.$$

4.2 computation of $c_2(s)$

Using the approximations of $(\theta(s_i), \theta'(s_i))$ given so far, we can now use (equation 2) to approximate the function $c_2(s)$. To accomplish this, we need the following formulas for approximating the derivatives of any given function $g(s)$:

i) for the derivative at $s_1 = 0$ we use:

$$g'(s_1) \approx \frac{\gamma_1 g(s_2) + (1 - \gamma_1) g(s_1) - g(s_3)}{\delta_1}, \tag{3}$$

where

$$h_1 = s_2 - s_1, \quad h_2 = s_3 - s_2,$$
$$\gamma_1 = \left[\frac{h_1 + h_2}{h_1} \right], \quad \delta_1 = \frac{h_2}{h_1}(h_1 + h_2).$$

ii) To approximate the derivative at s_n we use:

$$g'(s_n) \approx \frac{g(s_{n-2}) - (1 - \gamma_n) g(s_n) - \gamma_n g(s_{n-1})}{\delta_n}, \tag{4}$$

where

$$h_n = s_n - s_{n-1}, \qquad h_{n-1} = s_{n-1} - s_{n-2},$$
$$\gamma_n = \left[\frac{h_{n-1} + h_n}{h_n}\right]^2, \quad \delta_n = \frac{h_{n-1}}{h_n}(h_{n-1} + h_n).$$

iii) To approximate the derivative at the intermediate points s_i, $2 \le i \le n$-1, we use:

$$g'(s_i) \approx \frac{g_{i+1} - g_{i-1}}{s_{i+1} - s_{i-1}}. \tag{5}$$

These formulas have an $\boldsymbol{O}(h^2)$ degree of approximation where

$$h = \max\{s_{i+1} - s_i \mid 1 \le i \le n-1\}.$$

We approximate $\hat{M}$ ($\theta'(s_i)$, s_i) with:

$$M_i = \hat{M}(\theta_i', s_i), \quad 1 \le i \le n.$$

For ease of notation, we write $c(s)$ in (equation 2) instead of $c_2(s)$. As $c(L) = 0$, we have upon setting $s = s_n$ in (equation 2), and using (equation 4), that

$$c_n = 0, \quad l = -\frac{M_{n-2} - (1-\gamma_n)M_n - \gamma_n M_{n-1}}{\delta_n}. \tag{6}$$

If we evaluate (equation 2) at s_1, use the value of l already computed, and the formula (equation 3), we get that

$$c_1 = -\frac{1}{\cos\theta_1}\left[\frac{\gamma_1 M_2 + (1-\gamma_1)M_1 - M_3}{\delta_1} + l\right]. \tag{7}$$

Finally, if we evaluate (equation 2) at s_i and use (equation 5), we have that:

$$c_i = -\frac{1}{\cos\theta_i}\left[\frac{M_{i+1} - M_{i-1}}{s_{i+1} - s_{i-1}} + l\right], \quad 2 \le i \le n-1. \tag{8}$$

Since $\mathbf{f}(s) = -\mathbf{c}'(s)$, we can use a spline to interpolate the c_i's, and then differentiate the spline to get approximations for the vertical component of the external force **f**.

5. Results

We now specify the constitutive function $\hat{M}$ in (2.9). For the present paper we use the linear (in μ) relation:

$$\hat{M}(\mu, s) = (EI)(s)\mu. \tag{9}$$

In this equation, $E(s)$ is the Young modulus of the material of the bar or fiber at s, and $I(s)$ is the area moment of inertia for the cross sections of the bar at s. When the cross sections of the bar are circular with radius $a(s)$ at s, then the area moment of inertia is given by the equation:

$$I(s) = \frac{\pi}{4}a^4(s).$$

In Figure 1a we show the laboratory picture of the deformed fiber that we work with. This fiber is a composite of carbon nanotubes with a polymer. The deformation of the fiber could be accounted to a photo-actuation effect when the fiber is irradiated with an external light source[8]. For this fiber we have the following approximate values for *a, E* (assumed constant):

$$a = 0.5\times 10^{-7}\ \text{m}\ (100\text{nm diameter}),$$
$$E = 1.15\ \text{MPa} = 1.15\times 10^{6}\ \frac{\text{N}}{\text{m}^2}.$$

This value of *E* corresponds to a 2 wt% composite with an approximate density of 1mg/mm^3 [11].

In Figure 1b we show a digitized deformation version of Figure 1a. Finally, in Figure 2 we show the graph of the computed vertical component f_2 of the external body force **f** induced by photo-actuation. The data for this graph is obtained from the computed c_i's according to the formulas (6)-(8). Note that the maximum value of f_2 is at $s = 0$ which is where the fiber is attached, and diminishes as *s* increases (although not monotonically). The average value of this component of force over the whole *s* interval is given by:

$$\frac{1}{L}\int_0^L f_2(s)\,\mathrm{d}s \approx 2.1830\times 10^{-11}\ \text{N},$$

where $L = s_n \approx 4.976 \times 10^{-4}$ m. This positive value for the average is consistent with an average bending of the fiber in the positive vertical direction.

Once we have a working model for computing the effects of photo actuation on the fiber, we can conduct experiments using the model. For example, in Figure 3 we show the effect of varying the Young modulus *E* on the average value of the external force and the external couple *l* (units of torque per unit length or Newtons). These results could be used to predict photo actuation effects on fibers with varying concentrations (wt%) of the composite of carbon nanotubes and polymer in our case. Other possible experiments could be to study the effects of various cross sectional geometries on the computed average external force and couple.

6. Closing Remarks

Inverse problems are in general ill-posed. That is, in general they have no solution, and when they do, in general is not unique. In our case, by imposing some additional conditions on the solutions sought, we were able to solve the inverse problem to get an estimate of the photo-actuation effect on the fiber. The results show that the proposed method could be a very useful tool to study these photo-actuation effects on other fibers produced by the electro-spinning technique or any other method. It would be interesting to study the dependence of the external photo-actuation effect on light intensity and frequency, and on the various production parameters of the fibers. Another important aspect that requires further study is on the selection of the constitutive function in (equation 9), in particular, the possibility that this function on itself may depend on the parameters of intensity, frequency, etc..
Since the fiber deformations are in general three dimensional, it would be interesting and challenging to consider more general mechanical models for such deformations.

7. Acknowledgments

This research has been founded the NSF-PREM Program of the University of Puerto Rico at Humacao (Grant No. DMR-0934195).

8. References

1. Ahir, Samit V., and Eugene M. Terentjev. "Photomecanical actuation in polymer-nanotube composites." *Nature Materials*. 4. no. 6 (2005): 491-495.
2. Ahir, S. V., A.M. Squires, A.R. Tajbakhsh, and E. M. Terentjev. "Infrared actuation in aligned polymer-nanotube composites." *Physical Review*. B 73. no. 085420 (2006).

3. Antman, S. *Nonlinear Problems of Elasticity.* 2nd ed. New York: Springer, 2005.
4. Bar-Cohen, Y., and Q. Zhang. "Electroactive Polymer Actuators and Sensors." *MRS Bulletin*. 33. no. 03 (2008): 173-181.
5. Behl, M., M.Y. Razzaq, and A. Lendlein. "Multifunctional Shape-Memory Polymers." *Advanced Materials*. 22. no. 31 (2010): 3388-3410.
6. Burden, R., and J. Faires. *Numerical Analysis*. 9th ed. Brooks Cole, 2010.
7. Holzapfel, G.A., and R.W. Ogden. "On the Bending and Stretching Elasticity of Biopolymer Filaments."*Journal of Elasticity*. 104. no. 1-2 (2011): 319-342.
8. Meléndez, A., L. Santa, I. Ramos, J. Santiago-Avilés, E.M. Campo , and J.P. Crespo. "Electrospun Polymer/MWCNT Composite Fibers." *SPIE*. (2011).
9. Meng, H., and J. Hu. "A Brief Review of Stimulus-active Polymers Responsive to Thermal, Light, Magnetic, Electric, and Water/Solvent Stimuli." *Journal of Intelligent Material Systems and Structures*. 21. no. 9 (2010): 859-885.
10. Smela, E. "Conjugated Polymer Actuators." *MRS Bulletin*. 33. no. 03 (2008): 197-204.
11. Torres-Andrés, N. *Cálculo Distribución Espacial de CNT*. Proyecto NOMS, Marzo 2010.

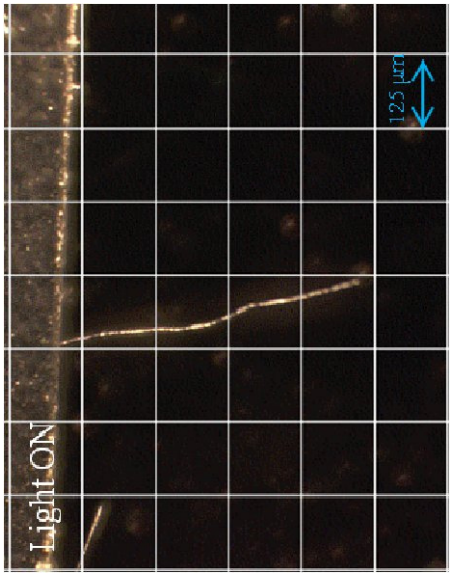

a) Deformed fiber of a carbon nanotube polymer composite.

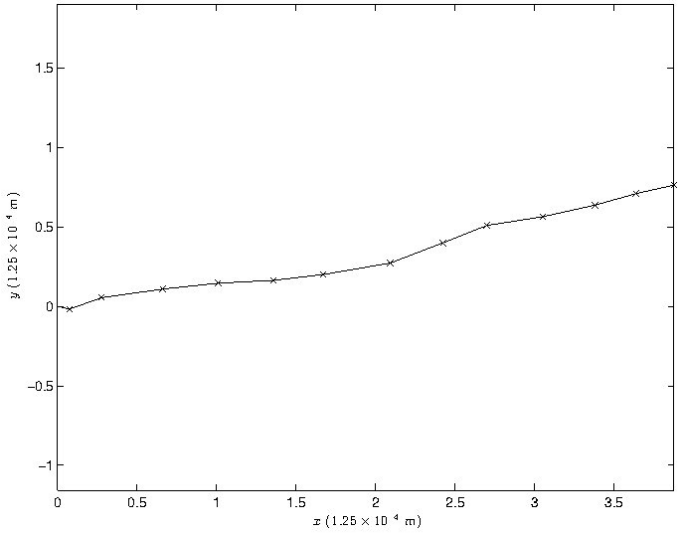

b) Digitized deformed fiber.

Figure 1: Deformed fiber

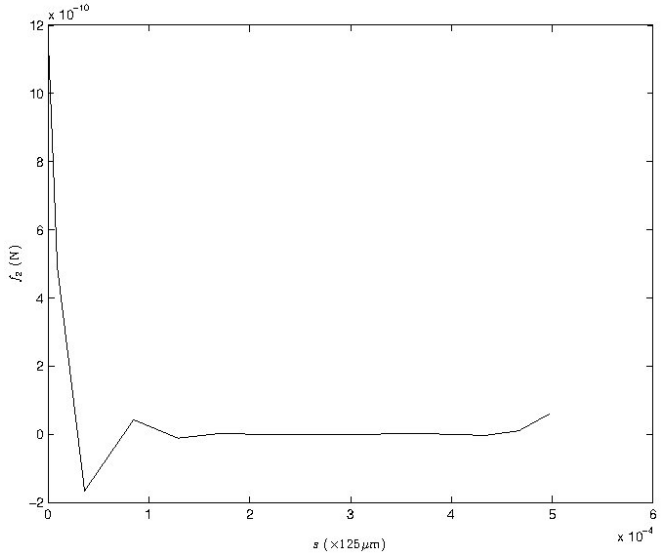

Figure 2: Vertical component of the external body force obtained by the inverse method.

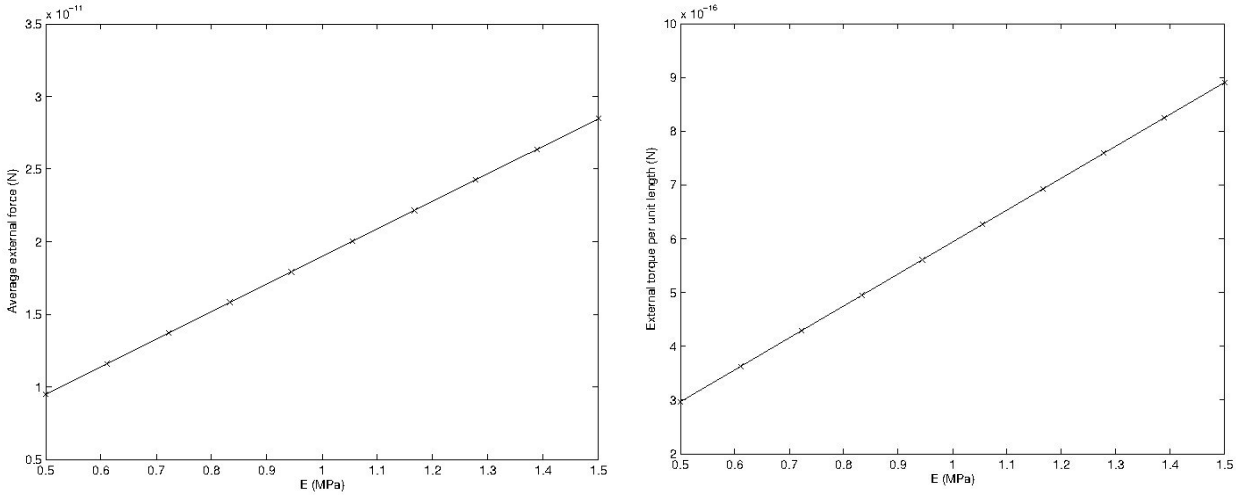

a) Average external force vs Young modulus. b) Average external torque vs Young modulus.

Figure 3: Effects of varying Young modulus on external average force and couple.